JOURNAL OF MATERIALS SCIENCE 28 (1993) 2169–2177

Preparation and optical properties of phase-change VO_2 thin films

SONGWEI LU, LISONG HOU, FUXI GAN
Shanghai Institute of Optics and Fine Mechanics, Academia Sinica, PO Box 800-216, Shanghai 201800, People's Republic of China

In this work, VO_2 thin films were prepared on three kinds of substrates by the sol–gel dip-coating method followed by heat treatment under vacuum. These thin films were analysed by x-ray diffraction (XRD) and X-ray photoelectron spectroscopy (XPS) techniques. The infrared and ultraviolet–visible spectra of the VO_2 thin films were also recorded during heating and cooling between room temperature and 100 °C. The experimental results show that VO_2 thin films thus prepared exhibit thermally induced reversible phase transition, and the largest changes in transmittance and reflectivity are approximately 58 and 25%, respectively, in the case of vacuum heat treatment at 400 °C and silica glass substrates. The refractive index (n) decreases and the absorption coefficient (k) increases when heating these thin films from room temperature to 100 °C, and vice versa for cooling. The reasons why the optical constants and infrared absorption spectra change so remarkably are discussed.

1. Introduction

It was well known that VO_2 exhibits a thermally induced reversible phase transition near 67 °C. This phenomenon was discovered for the first time in 1959 by Morin [1], whose results showed that the conductivity of VO_2 changed reversibly by two orders of magnitude while cooling and heating over a temperature range from 52 to 77 °C. Since then, the changes in the optical, electrical and magnetic properties of this material and their applications have been studied by a large number of investigators [2–4]. In 1971 Goodenough [5] proposed a band model based on crystal field theory to explain the mechanism of the monoclinic-to-tetragonal phase change. In the same year Roach [6] found that the reflectivity of VO_2 thin films prepared by reactive sputtering on glass substrates changed by 8% during the phase transition, and therefore he pointed out for the first time that VO_2 thin films can be used as a kind of optical disc medium. In 1986 Lee *et al.* [7] suggested that W-doped VO_2 thin films can be used as a sort of energy-efficient window.

A number of methods have been used to prepare VO_2 thin films, such as vacuum evaporation [8], r.f. sputtering [9], chemical vapour deposition and the sol–gel process [10]. However, most of the previous work focused on the phase transition phenomenon itself and its applications. Few systematic investigations have been conducted, especially for sol–gel-derived thin films. In this work VO_2 thin films were prepared by the sol–gel dip-coating method followed by heat treatment under vacuum. The phase change phenomenon was observed and the change in the optical properties of these VO_2 thin films was investigated.

2. Experimental procedure

2.1. Sample preparation

2.1.1. Preparation of sols

25 g tri-isopropoxyvanadyl [$VO(i\text{-}OC_2H_5)_3$; TRI Chemical Laboratory, Japan; 99.999% purity] was diluted to 100 ml with ethanol in a brown glass volumetric flask, and was then kept hermetically in a brown glass bottle (solution A). Water was diluted with ethanol at an H_2O/C_2H_5OH volume ratio of 1 : 49 (solution B). Transparent orange V_2O_5 sols were carefully prepared by the hydrolysis of the alkoxide with a $H_2O/VO(i\text{-}OC_2H_5)_3$ molar ratio of 2.0 (Fig. 1). Sols thus prepared and sealed hermetically in a brown bottle can remain transparent for nearly 3 months. Several drops of acetylacetone were added to stabilize the solution and the colour of the sols changed to purple. The sols can remain transparent for more than 6 months with the addition of acetylacetone. However sols prepared with a $H_2O/VO(i\text{-}OC_2H_5)_3$ molar ratio of 4.0 will precipitate 5 days after preparation.

2.1.2. Preparation of V_2O_5 thin films

As a viscosity-increasing reagent, hydroxypropylecellulose (HPC, 2.5 wt %, diluted by ethanol) was added into the sols at a volume percentage of 25%. The aim of the addition of HPC was to adjust the viscosity of the sols and increase the thickness of the films by one dip-coating operation (Fig. 2). The viscosity of the sols containing HPC decreased gradually with increased ageing time, possibly due to the slow reaction between HPC and the components of the sols. The precleaned substrates [silica glass, soda-lime–silica glass (i.e. slide glass) and monocrystalline silicon (1 1 1)] were dipped

0022–2461

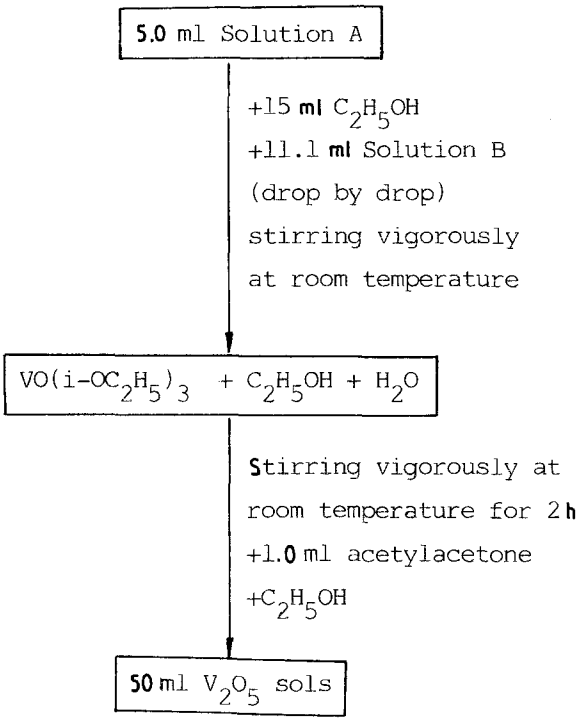

Figure 1 Schematic representation of the preparation process of V_2O_5 sols.

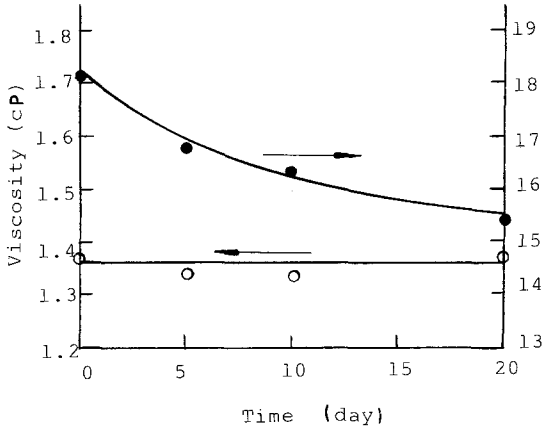

Figure 2 Viscosity of V_2O_5 sols (●) with or (○) without HPC as a function of time.

into the sols and pulled up at a constant speed of 11.6 cm min^{-1}. Each substrate was coated five times to increase the thickness of the film. The sol–gel dip-coating apparatus is well known generally for other films [11] and is illustrated elsewhere [12]. The coated substrates were then exposed to the atmosphere for 15 min before the next dipping. The as-prepared V_2O_5 thin films were orange-yellow in colour and of high surface quality.

2.1.3. Heat treatment

Grey-black VO_2 thin films were obtained by low vacuum (6.7 Pa) heat treatment at 400 or 500 °C for 2 h. Orange-yellow V_2O_5 thin films were obtained when they were heat treated in air at 250 or 500 °C for 2 h. Three samples were heat treated under vacuum at 100, 200 and 300 °C, respectively, for the purpose of comparison with those heated at high temperatures.

2.1.4. Preparation of VO_2 and V_2O_5 powders

By spreading the V_2O_5 sols on a glass sheet and then drying it, V_2O_5 gel powders were obtained. Grey-black VO_2 powders were obtained by heating the V_2O_5 gel powders at 500 °C for 2 h under vacuum conditions (6.7 Pa), whereas orange-yellow V_2O_5 powders were obtained by heating the V_2O_5 gel powders in air.

2.2. Techniques of the properties measurement

Transmittance spectra of VO_2 thin films in the region of 200–300 nm were recorded at room temperature and at 100 °C, using a Perkin–Elmer Lambda ultraviolet–visible–near–infrared spectrometer. The near-infrared transmittance–temperature hysteresis curves of these films at 2.0 μm were recorded by a 44 W infrared spectrometer. Infrared spectra of VO_2 powders between 4000 and 400 cm^{-1} during heating and cooling were recorded using a Perkin–Elmer 983G infrared spectrometer with a heat cell and a temperature controller. Surface XPS analysis was conducted using a Perkin–Elmer PHI-50 ESCA–SIMS–Auger spectrometer under high vacuum (1.3×10^{-7} Pa). For each kind of substrate used the films were analysed by XRD using a Rigau D/Max-A diffractometer. Differential scanning calorimetry (DSC) experiments were performed using a Rigau differential thermal analyser. The thickness of the thin films was measured with a Dektak stylus instrument.

2.3. Analyses of errors of measurement and calculation

In this work parameters such as the viscosity of the sols, thickness of the gel-derived thin films, transmittance and reflectivity of the thin films versus temperature were measured for three samples that were prepared under the same conditions. The data in the figures and tables are the average values of these measurement results. The maximum error of thickness, for example, was ± 2.5 nm, as the maximum resolution of the Dektak stylus instrument is 2.5 nm. The transmittance–wavelength curves, XRD, XPS and DSC measurements were carried out for three samples prepared under the same conditions.

The optical constants n and k of the gel-derived thin films were calculated by the optimum seeking method according to the relationship between R, T and n, k and d of the thin films:

$$R = R(n, k, d) \quad \text{and} \quad T = T(n,k,d) \qquad (1)$$

The best results were obtained in the case of $n \gg k$ or $n \ll k$ because of the least relativity between n and k. The method includes four steps. First, assume initial values of n_0 and k_0. Secondly, seek in the neighbourhood of n_0 and find the optimum refractive index

n_1, using $k = k_0$ and error $R = |R_c - R_m|$ as the evaluation function, where R_c and R_m are the calculated and measured reflectivities, respectively. Thirdly, seek in the neighbourhood of k_0 and find the optimum absorption coefficient k_1, using $n = n_1$ and error $T = |T_c - T_m|$ as the evaluation function, where T_c and T_m are the calculated and measured transmittances, respectively. Fourthly, rerun the above steps with n_0 and k_0 replaced by n_1 and k_1, and so on.

In this method, the errors of n and k derived from errors of R, T and d are shown in Table I. From the table, the errors in n and k are mainly derived from the error of R and less from the error of d. The optimum results are approached when the difference between n and k is very large. The optical constants n and k of VO_2 thin films before and after phase transition are presented in Table II. The data indicated are of low reliability because the difference between n and k in these cases is too small to meet the requirement of our calculations.

3. Results

3.1. Thickness of the gel-derived thin films

Figs 3 and 4 show the relationship between the thickness and the withdrawal times and square root of the withdrawal speed, respectively. It is seen that the film thickness increases with increasing dip-coating time and withdrawal speed.

3.2. XPS analyses of the gel-derived thin films after heat treatment

XPS analysis results of the surface composition are shown in Fig. 5 and Table III. It is demonstrated that vanadium exists as V^{5+} ion after heat treatment at 500 °C for 2 h in air; however, in the case of heat treatment above 400 °C under vacuum vanadium exists as V^{4+} ion, due to the lack of oxygen.

TABLE I Errors of n and k derived from errors of R, T and d of the thin films

Error of measurement (%)		Error of n and k[a] (%)
Reflectivity, R	1	1–6
Transmittance, T	1	0.5–4
Thickness, d	6	5–6
Different initial seeking region		1–2

[a] Calculated results by the optimum seeking method.

Fig. 6 shows the XPS spectrum of sample 2 at 90 °C under high vacuum (1.3×10^{-7} Pa). The valence state of vanadium ion is +4. However, the peaks of O(1s) and V($2p_{3/2}$) at 90 °C are wider than that at room temperature. The reason is that the chemical circumstance of all the ions in the thin films is changed due to the phase transition through heating. In this case no

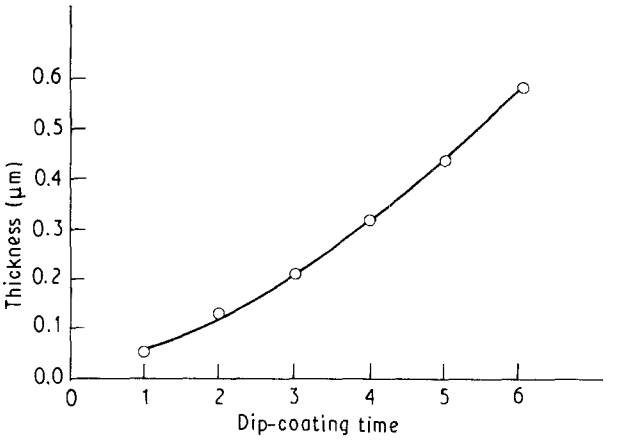

Figure 3 Relationship between the thickness of the thin films on silica glass substrates and the dip-coating times (withdrawal speed 11.6 cm min^{-1}).

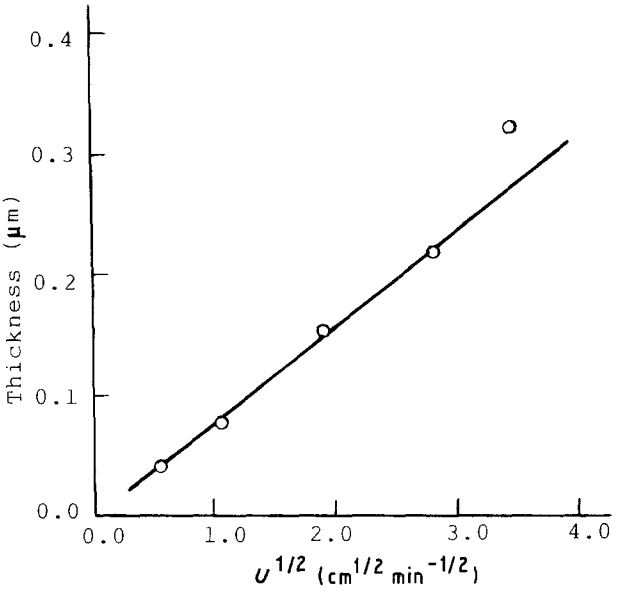

Figure 4 Relationship between the film thickness on silica glass substrates and the square root of withdrawal speed, $U^{1/2}$ (dip-coating four times).

TABLE II Optical constants of VO_2 thin films (85 nm thick) at 25 and 100 °C

Wavelength	Before phase transition				After phase transition			
(μm)	R (%)	T (%)	n	k	R (%)	T (%)	n	k
0.6	23.1	39.7	2.39	0.38	17.4	36.7	1.92	0.49
1.0	32.3	43.1	2.49	0.39	29.9	26.5	2.28	0.96
1.5	34.0	53.5	2.73	0.21	48.8	15.8	2.23[a]	2.53[a]
2.0	29.0	64.7	2.80	0.10	55.4	12.5		
2.5	23.4	68.2	2.81	0.16	42.3	10.4	2.61[a]	3.24[a]

[a] Data of low reliability due to the limitation of the calculation method.

peaks of other vanadium ions or vanadium metal (the peak position is at 511.95 eV) were found, suggesting that the vanadium valence state in this material does not change before and after phase transition.

3.3. XRD analyses of the gel-derived thin films after heat treatment

XRD patterns of the VO_2 thin films on three kinds of substrates are shown in Figs 7 and 8. It is clear that the films crystallized after vacuum heat treatment at 500 °C for 2 h. The films on monocrystalline Si(1 1 1) substrates were apparently rich in VO_2 crystals. The influence of Na_2O from the slide glass substrates is evinced by the corresponding diffraction patterns [10]. No crystallization peak was detected from the thin films on slide glass substrates after vacuum heat treatment at ≤ 400 °C. It is for this reason that the extent of crystallization is too small to be detected, or the vanadium oxide thin films heat treated at lower temperatures below 400 °C are amorphous. From the XRD patterns of VO_2 powders after vacuum heat treatment it is seen that the powders are polycrystalline.

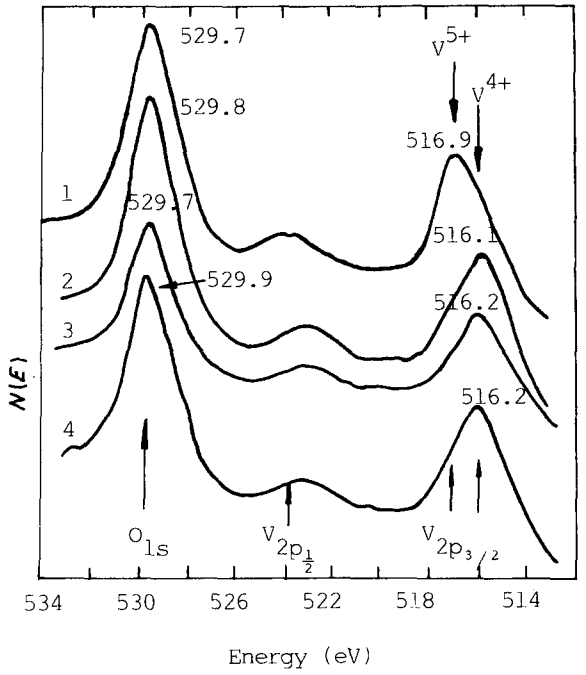

Figure 5 Surface XPS peaks of O_{1s} and V_{2p} of samples 1–4. All peaks are standardized with respect to standard C_{1s} peak. The standard $V^{5+}_{2p\,3/2}$ and $V^{4+}_{2p\,3/2}$ peaks being at 517.45 and 516.45 eV, respectively.

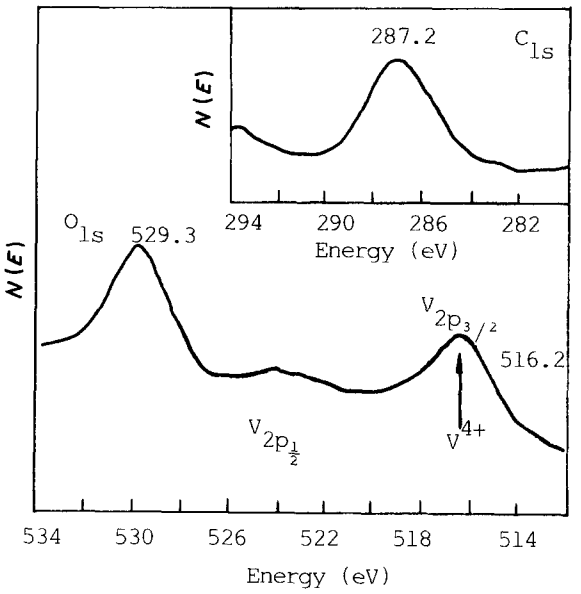

Figure 6 Surface XPS peaks of O(1s) and V($2p_{3/2}$) of sample 2 at 90 °C (under vacuum of 1.3×10^{-7} Pa), $O_{(1s)}$ and $V_{(2p)}$ peaks are standardized with respect to the standard C(1s) peak.

TABLE III XPS Surface composition analysis results of the sample prepared under different conditions

Sample no.	Substrate	Heat treatment conditions	Surface element			V valence	V oxide
1	Slide glass	500 °C/2 h in air	V	O	C	+5	V_2O_5
2	Slide glass	500 °C/2 h under 6.7 Pa	V	O	C	+4	VO_2
3	Slide glass	400 °C/2 h under 6.7 Pa	V	O	C	+4	VO_2
4	Silica glass	500 °C/2 h under 6.7 Pa	V	O	C	+4	VO_2
2[a]	Slide glass	500 °C/2 h under 6.7 Pa	V	O	C	+4	VO_2

[a] Sample 2 kept at 90 °C during the XPS measurement.

TABLE IV Infrared transmittance (in %) of VO_2 powders, VO_2 thin films and V_2O_5 thin films on monocrystalline Si(1 1 1) substrates at various temperatures

Measurement temperature (°C)	VO_2 thin films			VO_2 powders			V_2O_5 thin films		
	2.5 μm	4.0 μm	5.0 μm	2.5 μm	4.0 μm	5.0 μm	2.5 μm	4.0 μm	5.0 μm
20	64	77	86	12.4	16.2	18.5	67	76	64
60[a]	62	73	82	12.4	16.0	18.4			
100	25	33	41	4.6	9.6	12.4	68	75	63
60[b]	31	37	49	8.0	12.4	15.0			

[a] During heating and [b] during cooling.

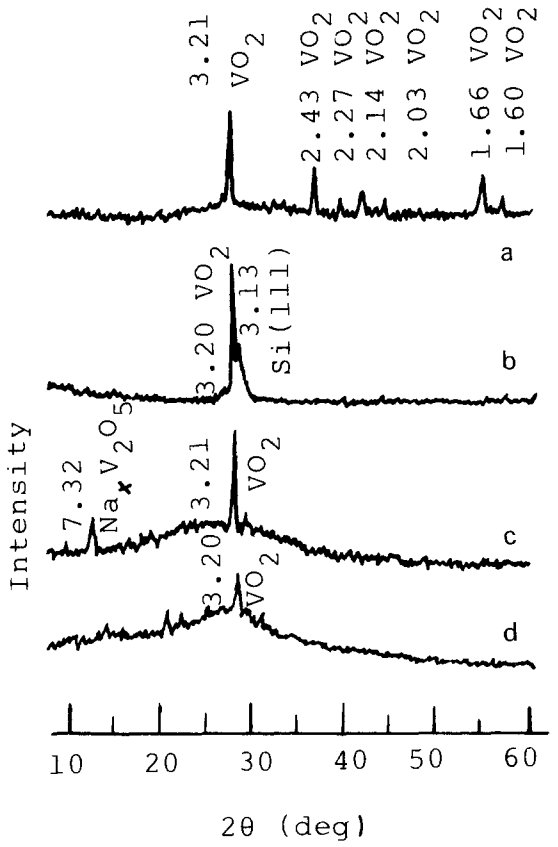

Figure 7 XRD patterns of (a) VO_2 powders and the gel-derived VO_2 thin films on three kinds of substrates: (b) silicon (1 1 1), (c) slide glass substrates and (d) silica glass substrates.

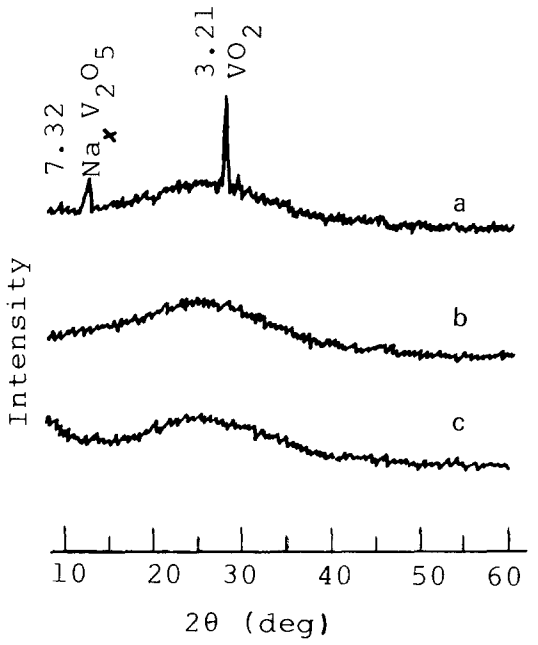

Figure 8 XRD patterns of VO_x thin films on slide glass substrates (heat treated at different temperatures for 2 h under 6.7 Pa): (a) 500 °C, (b) 400 °C and (c) 100 °C.

3.4. Thermally induced reversible phase transition

In the present work, the thermally induced reversible phase transition phenomenon was observed during heating and cooling. Figs 9–11 show the transmittance and reflectivity of VO_2 thin films as a function of

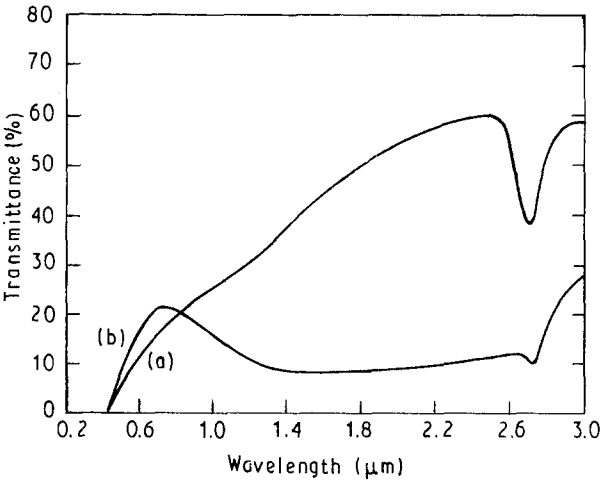

Figure 9 Transmittance curves of VO_2 thin film (about 170 nm thick) on silica glass substrate at (a) room temperature and (b) 100 °C (heat treated at 500 °C for 2 h under 6.7 Pa).

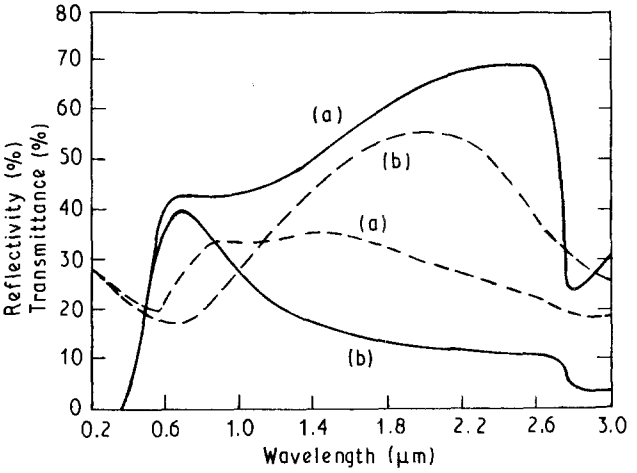

Figure 10 (——) Transmittance and (– – –) reflectivity curves of VO_2 thin film (about 85 nm thick) on silica glass substrate at (a) room temperature and (b) 100° C (heat treated at 400 °C for 2 h under 6.7 Pa).

wavelength at 25 and 100 °C. The infrared absorption peaks near 2.7 μm in these figures are attributed to water absorption. The reversible transmittance–temperature hystereses due to the phase transition of VO_2 thin films on monocrystalline Si(1 1 1) are shown in Fig. 12. The transmittance – temperature hystereses of VO_x ($2.0 \leq x < 2.5$) thin films on slide glass substrates heat treated under different conditions are shown in Fig. 13.

The experimental results indicate that the optical properties of VO_2 thin films change remarkably due to the phase transition, the extent of the change in optical properties and the transition temperature (T_t) are different for thin films on different substrates, of different thickness and heat treated under different conditions. The largest changes in transmittance and reflectivity are approximately 58 and 25%, respectively, in the case of vacuum heat treatment at 400 °C and silica glass substrates (Fig. 10). However, for thin films heat treated at 250 °C in air for 2 h, almost no difference in transmittance could be detected between room temperature and 100 °C (Table IV). Meanwhile,

almost no difference in transmittance and no reversible hysteresis could be observed when these thin films were treated under vacuum conditions below 400 °C (Fig. 13).

3.5. The optical constants of VO_2 thin films before and after phase transition

The optical constants, n and k, of VO_2 thin films were calculated using the vertical reflectivity (R), vertical transmittance (T) and film thickness (d) data taken from Fig. 10 and are listed in Table II. The calculation method was as detailed above. It is clear from Table II that n decreases and k increases when heating the sample from room temperature to 100 °C.

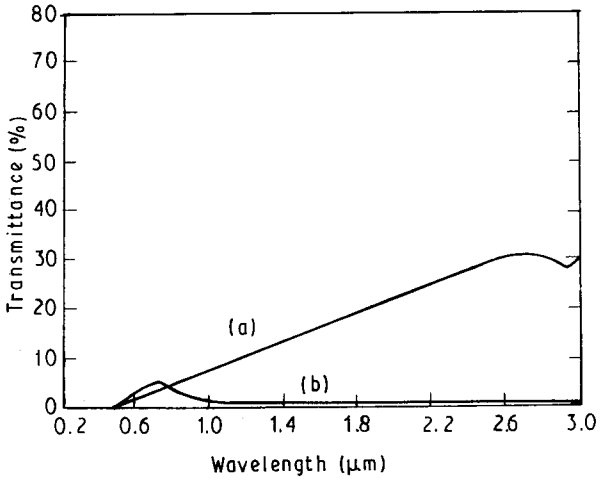

Figure 11 Transmittance curves of VO_2 thin film (about 290 nm thick) on slide glass substrate at (a) room temperature and (b) 100 °C (heat treated at 500 °C for 2 h under 6.7 Pa).

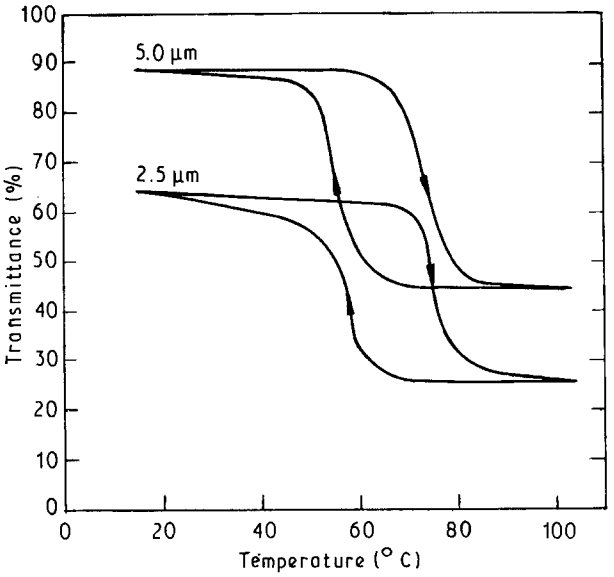

Figure 12 Infrared transmittance–temperature hystereses of VO_2 thin films (about 440 nm thick) on monocrystalline silicon (1 1 1) substrates.

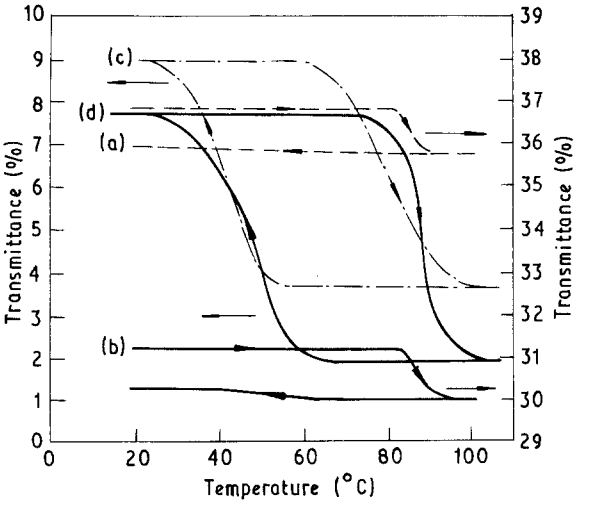

Figure 13 Transmittance–temperature hystereses at 2.0 μm of VO_x thin films on slide glass substrates (heat treated at different temperatures for 2 h under 6.7 Pa): (a) 200 °C, (b) 300 °C, (c) 400 °C and (d) 500 °C.

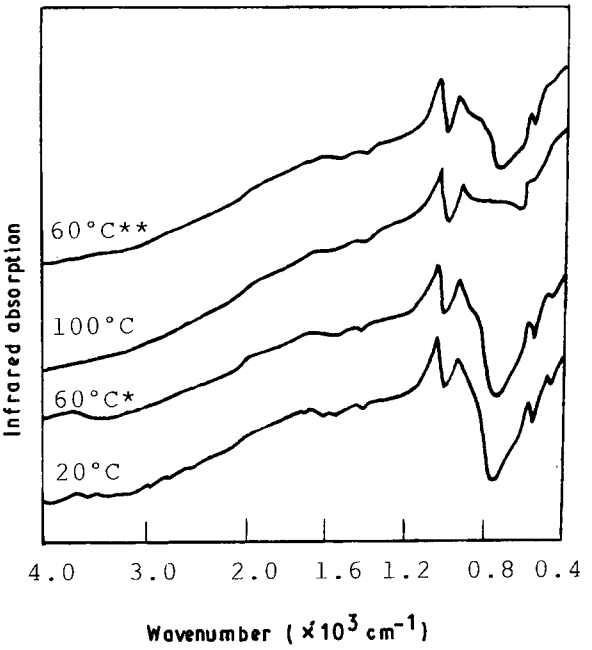

Figure 14 Infrared spectra of VO_2 powders during heating (*) and cooling (**).

3.6. Infrared absorption spectra

Fig. 14 shows the infrared absorption spectra of the VO_2 powders between 4000 and 400 cm^{-1} during heating and cooling. The spectra show that due to the phase change, the transmittance changes reversibly, and the absorption peaks at 744, 542 and 460 cm^{-1} disappeared gradually during heating, these peaks appearing again during cooling. However, the peaks at 990 and 606 cm^{-1} remained stable during heating and cooling.

3.7. DSC curves of the VO_2 powders

Fig. 15 shows the DSC curves of V_2O_5 powders and VO_2 powders between room temperature and 120 °C.

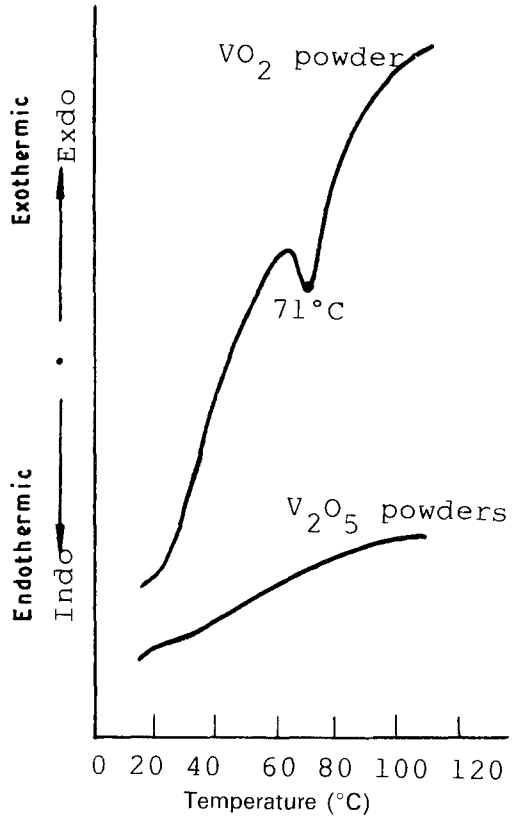

Figure 15 DSC curves of V_2O_5 and VO_2 powders prepared by the sol–gel method (heating rate 10 °C min^{-1}).

It is seen that there was no change in the DSC curve of V_2O_5 powders, whereas for VO_2 powders, there was an endothermic phase transition.

4. Discussion

4.1. The thickness of the gel-derived thin films

When using sols of low capillary number as the coating solutions, the thickness of one dip-coating operation (t_p) is given by the Landau–Levich expression in the form used by Yang [12, 13]

$$t_p = 0.944(N_{Ca})^{1/6}(\eta U/\rho g)^{1/2} \quad (2)$$

where N_{Ca} is surface capillary number, $N_{Ca} = \eta U/\sigma$, η being the dynamic viscosity, U the withdrawal speed and σ the surface tension of the solution, ρ and g are the density of the solution and the gravitational acceleration, respectively.

For a certain system (η, σ and ρ are constants) the thickness depends on U. The experiments of Schroeder [14] revealed that all suitable solution followed the same relationship, the coating thickness showing an approximate dependence on the withdrawal speed to the power two-thirds. Yoldas and O'Keffe [15] and Mukherjee [16] found a square root power relationship between t_p and U, and Sakka *et al.* [17] obtained a relationship to a power in the range 0.52–0.62. It is obvious from Equation 2 that t_p is approximately proportional to $U^{1/2}$ if N_{Ca} is very small. This is in good agreement with the experimental data in the case of low solution viscosity and low withdrawal speed.

In the present work the relationship between the thickness and the withdrawal speed fits Equation 2 well because of the low withdrawal speed (< 9 cm min^{-1}, see Fig. 14), i.e. low N_{Ca}. It is suggested that the Lendau–Levich expression agrees well with the experimental data not only in the case of one dip-coating operation, but also in the case of multiple dip-coating operations under certain conditions.

4.2. Relationship between the thermally induced reversible phase transition and heat treatment conditions of the films

As shown above (Figs 9–13 and Table IV), the phase transition difference occurs during heating and cooling of the thin films on the same kind of substrates, of the same thickness, but heat treated under different conditions. The reasons are as follows. First, thin films prepared by the sol–gel technique have lower density than those prepared by another method such as vacuum evaporation [7] or r.f. sputtering [8]. In the case of gel-derived vanadium oxide thin films, boundaries between the [VO_6] groups and the pores exist and supplementary boundary energy occurs for the as-coated films. When the films are heat treated under different conditions, the pores in the films collapse to different extents. Therefore, the phase transition is affected by the existing supplementary boundary energy. The chemical matching of V and O in the thin films is another reason. In the films heat treated in air, no VO_2 was formed, and no phase change can occur. In the films heat treated under vacuum conditions, V_2O_5 was reduced to VO_x ($2.0 \leq x < 2.5$) at high temperatures. The degree of the reduction was different at different heat treatment temperatures under a particular vacuum condition. The higher the temperature, the more complete the reduction and the greater the proportion of VO_2 in the thin films, and the lower the transmittance of the thin films at room temperature. The phase transition occurred in the thin films heat treated above 400 °C under low vacuum. This is clearly shown in Fig. 13. Finally, the extent of crystallization occurring in the thin films affects the phase transition. The higher the heat treatment temperature, the larger the crystal grain of vanadium oxide. Therefore, the extent of phase transition is different due to the different extent of crystallization. The last two reasons were demonstrated by the experiments of Fukuma *et al.* [18]. They found that the extent of reflectivity change of $VO_{2.003}$ thin films (heat treated at 450 °C for 4 h in flowing N_2, crystal grain size about 50 nm) is larger than that of $VO_{2.006}$ thin films (heat treated at 500 °C for 4 h in flowing N_2, crystal grain size 250 nm).

4.3. Relationship between the optical constants and the phase transition of VO_2

As noted above, VO_2 exhibits a thermally induced reversible phase transition near 67 °C. Below the transition temperature (T_t) the [VO_6] octahedron in the VO_2 structure is distorted because of the splitting of the 3d-orbit energy level of V^{4+} ions in the

octahedral crystal field, therefore VO_2 is in a monoclinic structure similar to that of MoO_2. Above T_t the distortion disappears, so VO_2 is in the tetragonal rutile structure of TiO_2. This structural change of VO_2 during heating and cooling results in the change of optical, electrical and magnetic properties.

From Table II it is known that n decreases and k increases when heating the sample from room temperature to 100 °C. The changes in optical constants during phase transition can be explained based on the relationship between the optical constants and materials structure.

According to Maxwell's electromagnetic theory and the classical mechanics, the above relationship can be expressed as

$$\frac{n^2-1}{n^2+2}\frac{3\varepsilon_0}{N} = \frac{\alpha\rho}{M} \quad (3)$$

where M is the molecular weight, ρ is the density, α is the polarizability, n is the refractive index, and N and ε_0 are Avogadro's number and vacuum permittivity, respectively. From Equation 3 it is known that the refractive index increases with increasing ion accumulation density and ion polarizability.

As is known, the lengths of V–O bonds (d_{V-O}) are different when $[VO_6]$ is distorted in the octahedral crystal field in the case of lower temperature below T_t. The values of d_{V-O} between V^{4+} ion and O^{2-} are 0.126, 0.186, 0.187, 0.201, 0.203 and 0.205 nm, respectively, in the monoclinic structure [19]. Polarization occurs when d_{V-O} is less than the sum of the radii of the V^{4+} ion and O^{2-} ion ($R_{V-O} = r_{V^{4+}} + r_{O}^{2-}$ = 0.200 nm). The greater the difference between d_{V-O} and R_{V-O}, the more the polarization and the larger the polarizability. However, in the case of VO_2 at high temperature above T_t, $[VO_6]$ becomes tetragonal in structure and d_{V-O} equals 0.194 nm, very close to R_{V-O}. Therefore, the polarizability of monoclinic VO_2 is larger than that of tetragonal rutile VO_2. As the ion accumulation density is similar for these two different structures, the refractive index of VO_2 decreases when VO_2 changes from monoclinic structure at low temperature to tetragonal rutile structure at high temperature due to the thermally induced phase transition.

4.4. The reason of the remarkable change of infrared absorption spectra

In the tetragonal rutile VO_2 structure, $[VO_6]$ belongs to the highly symmetrical O_h group. Simplified vibration modes of octahedral molecule XY_6 of O_h group are given in Fig. 16. In this case symmetrical stretching vibration modes $\nu_1(A_{1g})$, $\nu_2(E_g)$, $\nu_5(F_{2g})$ and $\nu_6(F_{2\mu})$ would not give rise to a dipole moment change of full octahedron and therefore these vibrations are infrared-inactive and have no absorption peaks in the infrared spectrum. However, vibration modes $\nu_3(F_{1\mu})$ and $\nu_4(F_{1\mu})$ give rise to a dipole moment change and have absorption peaks in the infrared spectrum. This is the reason why some absorption peaks disappear in the infrared spectra of VO_2 powders above T_t as shown in Fig. 14.

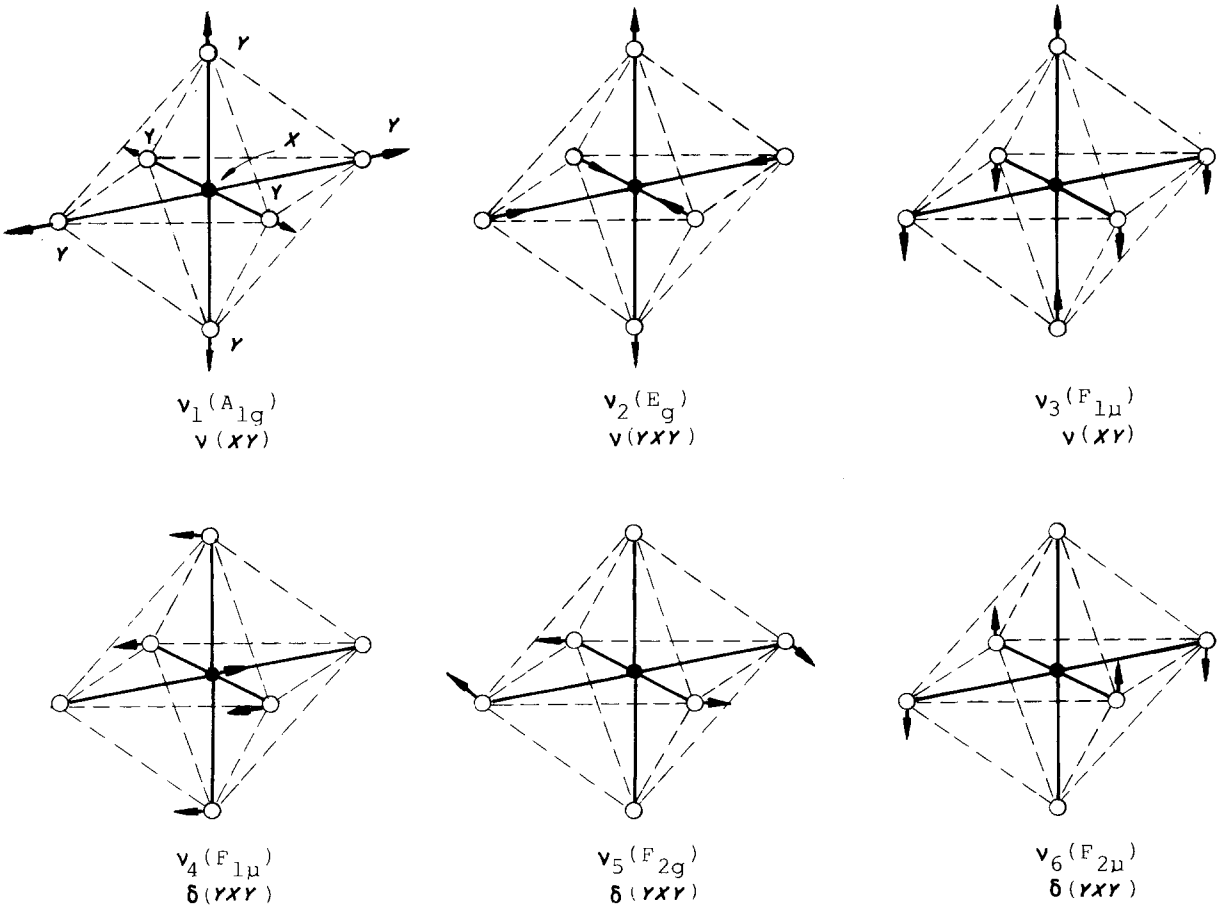

Figure 16 Simplified vibration modes of octahedral molecule XY_6 of O_h group: (○) O and (●) V.

Below T_t the $[VO_6]$ octahedron distorts, and all these vibration modes (ν_1 to ν_6) give rise to a dipole moment change, they are infrared-active and all of these absorption peaks appear in the infrared spectrum.

5. Conclusion

VO_2 thin films exhibiting thermally induced reversible phase change can be prepared by the sol–gel dip-coating method and heat treatment under vacuum. The optical properties and optical constants of the thin films change remarkably during heating and cooling between room temperature and 100 °C. The largest changes in transmittance and reflectivity are approximately 58 and 25%, respectively, in the case of vacuum heat treatment at 400 °C and silica glass substrates. The change in optical constants is due to the polarizability change during structural transition between monoclinic VO_2 and tetragonal rutile VO_2. Above the phase transition temperature, some infrared absorption peaks of VO_2 powders disappear because of their infrared-inactive vibration of the highly symmetrical octahedral structure.

References

1. F. J. MORIN, *Phys. Rev. Lett.* **3** (1959) 34.
2. E. N. FULS, D. H. HENSLER and A. R. ROSS, *Appl. Phys. Lett.* **10** (1967) 199.
3. W. PAUL, *Mater. Res. Bull.* **5** (1970) 691.
4. D. D. EDEN, *Proc. SPIE* **185** (1979) 97.
5. J. B. GOODENOUGH, *J. Solid St. Chem.* **3** (1971) 490.
6. W. R. ROACH, *Appl. Phys. Lett.* **19** (1971) 453.
7. J. C. LEE, G. V. JORGENSON and R. J. LIN, *Proc. SPIE* **692** (1986) 2.
8. G. A. NYBERG and R. A. BUHRMAN, *J. Vacuum Sci. Technol.* **A2** (1984) 301.
9. T. E. PHILLIPS, R. A. MURPHY and T. O. POEHLER, *Mater. Res. Bull.* **22** (1987) 1113.
10. C. B. GREENBERG, *Thin Solid Films* **110** (1983) 73.
11. H. DISLISH and E. HUSSMANN, *ibid.* **77** (1981) 129.
12. C.-C. YANG, J. Y. JOSEFOWICZ and L. ALEXENDRU, *ibid.* **74** (1980) 117.
13. L. D. LANDAU and V. G. LEVICH, *Acta Physicochim. URSS* **17** (1942) 41.
14. H. SCHROEDER, *Phys. Thin Films* **5** (1969) 87.
15. B. E. YOLDAS and T. W. O'KEEFE, *Appl. Opt.* **18** (1979) 3133.
16. S. P. MUKHERJEE, in "Ultrastructure Processing of Ceramics, Glasses and Composities", edited by L. L. Hench and D. R. Ulrich (1984) 178.
17. S. SAKKA, K. KAMIYA, K. MAKITA and Y. YAMAMOTO, *J. Non-Cryst. Solids* **63** (Wiley, New York, 1984) 223.
18. M. FUKUMA, S. ZEMBUTSU and S. MIYAZAWA, *Appl. Opt.* **22** (1983) 265.
19. R. HECKINGBOTTOM and J. W. LINETT, *Nature* **194** (1962) 678.

Received 25 November 1991
and accepted 2 September 1992